

Extrapolated long-term stability of titanium dioxide nanoparticles and multi-walled carbon nanotubes in artificial freshwater

Andrea Brunelli · Alex Zabeo · Elena Semenzin ·
Danail Hristozov · Antonio Marcomini

Received: 24 July 2015 / Accepted: 5 April 2016 / Published online: 18 April 2016
© Springer Science+Business Media Dordrecht 2016

Abstract Long-term stability of two engineered nanomaterials (ENMs), i.e., the inorganic n-TiO₂ and the organic Multi-Walled Carbon Nanotubes (MWCNTs), dispersed in artificial freshwater (5–100 mg l⁻¹), was investigated from short-term settling velocity, particle size distribution, and surface charge. Hydrodynamic diameter and ζ-pot, calculated by means of dynamic and electrophoretic light scattering, respectively, qualitatively indicated a general ENMs dispersion instability over 1 h time. Sedimentation results, obtained by centrifugal separation analysis using the LUMiSizer over approx. 30 min analysis time, allowed to estimate the quantitative long-term (over 30 days) stability of ENMs. Settling data fitted satisfactorily with a first-order kinetic equation (R^2 in the range of 0.918–0.989). The settling rate constant k values extrapolated at gravity spanned one order of magnitude, i.e., from 7.21×10^{-5} to $4.12 \times 10^{-4} \text{ s}^{-1}$, and with the increasing of initial ENMs concentration. Sedimentation velocities were

in good agreement with short- to long-term literature data (7.8×10^{-2} – $1.7 \times 10^{-1} \text{ m day}^{-1}$ vs. 5×10^{-4} – $3 \times 10^{-1} \text{ m day}^{-1}$ for n-TiO₂ and 5.9×10^{-2} – $3.4 \times 10^{-1} \text{ m day}^{-1}$ vs. 2×10^{-1} – 1.2 m day^{-1} for MWCNTs). n-TiO₂ showed a higher long-term stability with respect to MWCNTs (average: $1 \times 10^{-1} \pm 3.4 \times 10^{-2} \text{ m day}^{-1}$ instead of $1.7 \times 10^{-1} \pm 1.1 \times 10^{-1} \text{ m day}^{-1}$, respectively).

Keywords Engineered nanomaterials · Environmental exposure · Sedimentation kinetics · Long-term stability estimation · Centrifugal separation analysis

Introduction

Unique physico-chemical properties of engineered nanomaterials (ENMs) with respect to the conventional bulk material have prompted the development of nanotechnology-based consumer products in many fields, including medicine, cosmetics, paints and coatings, electronics, textiles and sport items, food packaging, and energy storage (Piccinno et al. 2012). As a consequence, the potential environmental release and the resulting exposure to ENMs along their life cycle are expected to constantly increase (Farré et al. 2009; Nowack et al. 2012; Pettitt and Lead 2013). Based on environmental exposure scenarios, water is one of the main compartments where ENMs can be

Electronic supplementary material The online version of this article (doi:10.1007/s11051-016-3412-3) contains supplementary material, which is available to authorized users.

A. Brunelli · A. Zabeo · E. Semenzin ·
D. Hristozov · A. Marcomini (✉)
Department of Environmental Sciences, Informatics and
Statistics, University Ca' Foscari of Venice, Via delle
Industrie 21/8 c/o INCA - VEGAPARK, Marghera,
30175 Venice, Italy
e-mail: marcom@unive.it

released (Nowack et al. 2014). Similar to colloidal particles, ENMs in a fluid become dispersed as solid particles in a continuous medium, which leads to the formation of a dynamic and heterogeneous system. Classical colloid chemistry addressed the issue of colloidal suspension stability by applying the Derjaguin–Landau–Verwey–Overbeek (DLVO) theory (Dahirel and Jardat 2010), which combines two opposite forces: van der Waals attraction (i.e., sum of dipole–dipole forces, inductive forces, and dispersion forces) and electrostatic repulsion forces (Loux et al. 2011). The colloidal stability is observed only when the electrostatic forces dominate, while particles are likely to aggregate and thus settle out if attractive forces prevail. The stability of a colloidal system was experimentally investigated by applying an electrical field and measuring the movement of solid particles in dispersion (Hunter 1988). By an optical detection system, electrophoretic light scattering (ELS) was developed and used for characterizing surface charges of colloidal particles (Takeuchi et al. 1997; van der Zande et al. 2000). Depending of particles' charge, the recorded signal of the movements of particles can shift to different frequencies and then can be converted to electrophoretic mobility and to Zeta potential (ζ -pot), using the Smoluchowski equation (Jiang et al. 2009). A ζ -pot of at least ± 30 mV is normally required to achieve a stable colloidal dispersion. The use of this technique has also recently been extended to gather information on the stability of different ENMs dispersions (Suttiponparnit et al. 2011; Zhang et al. 2008).

The DLVO theory was reported in several studies to interpret experimental observations of ENMs agglomeration behavior (Buettner et al. 2010; Liu et al. 2011b; Liu and Hurt 2010), as well as to predict the agglomeration behavior of ENMs in liquids (Liu et al. 2011a). Even if a good agreement between the theory and experimental results was shown, some authors suggested that DLVO theory may have to be revised to be applied to ENMs, mainly because of different physico-chemical properties shown by ENMs in comparison with chemicals (Dahirel and Jardat 2010; Hotze et al. 2010). Moreover, DLVO theory has never been successfully used for complex matrices (Lowry et al. 2010).

Similar to colloidal particles, upon release into the environment, intrinsic physico-chemical properties of ENMs as well as the specific environmental conditions

mainly determine the fate and behavior of ENM (Hartmann et al. 2014; Wiesner et al. 2009). Therefore, a comprehensive characterization of all the processes affecting the ENMs system stability is needed. Among all, transformation processes, such as surface modification, homo- and hetero-aggregation, and transport processes, i.e., advection and sedimentation, have been identified as key factors to affect fate and behavior of ENMs in the aquatic environment (Quik et al. 2014a). Sedimentation and aggregation kinetics of different ENMs in several media have been investigated by numerous studies, combining experimental and numerical approaches (Afrooz et al. 2013; Brunelli et al. 2013; Chen and Elimelech 2006; Chowdhury et al. 2013; Gambinossi et al. 2015; Keller et al. 2010; Liu et al. 2012; Schwarzer and Peukert 2005; Zhang et al. 2012). In parallel, modeling approaches for estimating environmental exposure concentration of ENMs have been published (Arvidsson et al. 2011; Gottschalk et al. 2010; Mueller and Nowack 2008; Praetorius et al. 2012; Quik et al. 2011), including also key parameters for developing fate and exposure models for ENMs, i.e., sedimentation rates and non-settling fractions in natural waters and hetero-aggregation rates between ENMs and natural colloids (Quik et al. 2014a, b; Van Koetsem et al. 2015).

Experimental work performed so far on the sedimentation behavior of ENMs in dispersion was carried out with one of the following methods: (i) small angle neutron scattering (SANS), to estimate the concentration of silica nanoparticles and thus the settling velocity, at the top and near the bottom of the cuvette, just above the settled particles (Jarvie et al. 2009); (ii) molecular spectroscopy (Battin et al. 2009; Brunelli et al. 2013; Chinnapongse et al. 2011; Keller et al. 2010; Kennedy et al. 2008; Phenrat et al. 2006; Tiraferri et al. 2008), to measure the absorbance of ENMs over time, approx. at the middle of the cuvette, and thus to obtain the ENMs concentration by applying the Lambert–Beer's law, in order to finally calculate the sedimentation rates of ENMs in dispersion; (iii) inductively coupled plasma mass spectrometry (ICP-MS), as reported by Quik et al. (2010, 2012, Quik et al. 2014b) and Van Koetsem et al. (2015), to determine the concentration of inorganic ENMs over time, taking an aliquot from the middle of a dispersion at different times (i.e., up to 15 days), thus providing the sedimentation velocity of each ENM by fitting the experimental data with a first-order decay equation.

In summary, according to the current state of the art, fate and behavior of ENMs in dispersions were studied at gravity, over no more than 15 days and in a narrow region of the total volume investigated, by using time-consuming techniques. Adeleye and Keller (2014) and Schwyzer et al. (2012) were the only studies investigating the long-term colloidal stability of carbon nanotubes in water dispersions. Sedimentation kinetics for some ENMs were quantitatively calculated only by Brunelli et al. (2013), Quik et al. (2014b), and Van Koetsem et al. (2015), but no standardized protocols have been provided to carry out the characterization of the long-term stability of ENMs in dispersion. Predicted environmental concentrations of ENMs and available ecotoxicological data at realistic environmental concentrations (i.e., $\text{ng-}\mu\text{g l}^{-1}$) suggest that ENMs can cause sub-lethal and long-term effects (Farré et al. 2009; Ramsden et al. 2013; Villarreal et al. 2014). Therefore, experimental data on the long-term stability of ENMs is needed, in order to deeply understand the real exposure and effects of ENMs during chronic ecotoxicological testing as well as to feed fate and long-range transport modeling to support environmental risk assessment.

The aim of this work was to study the long-term stability (over 30 days) in artificial freshwater of both the inorganic titanium dioxide nanoparticles (n-TiO_2) P25 and the organic multi-walled carbon nanotubes (MWCNTs) NC7000, by short-time (no more than 1 h) measurements. The centrifugal separation analysis (CSA) method, using the Multi-wavelength Dispersion Analyzer, based on STEPTM technology (space and time resolved extinction profiles), according to ISO/TR 13,097:2013, was employed to calculate the sedimentation kinetics of dispersed ENMs. n-TiO_2 and MWCNTs were selected as models representative of spherical inorganic and tube organic ENMs, respectively, since they are widely used in e.g., coatings, paints, personal care, and cosmetic products (n-TiO_2) as well as in electronics, transports, sport, and leisure products (MWCNTs), and thus may reach the environment at different life cycle stages, either unaltered or, most likely, significantly transformed (Al-Kattan et al. 2014). This work focused specifically on transport processes of ENMs and, in particular, on sedimentation kinetics, because environmental fate and behavior of n-TiO_2 and MWCNTs are mainly affected by sedimentation, in addition to homo- and

hetero-aggregation/agglomeration (Hartmann et al. 2014).

Materials and methods

Characterization of pristine ENMs

The inorganic Aeroxide[®] P25 titanium dioxide nanopowder (n-TiO_2), obtained from Evonik Degussa (Germany), and the organic NanocylTM NC7000 multi-walled carbon nanotubes (MWCNT), received from Nanocyl s.a. (Belgium), were characterized by means of dynamic light scattering (DLS), ELS, and CSA. P25 powder (declared average particle size: 21 nm) is a mixture of approx. 80 % anatase and 20 % rutile, with 99.5 % purity, $50 \pm 15 \text{ m}^2 \text{ g}^{-1}$ as surface area, and a bulk density of 3.8 g cm^{-3} . Primary characterization of P25 is reported in our previous work (Brunelli et al. 2013). NC7000 powder has an average size diameter of 9.5 nm, with 1.5 μm length, declared as amorphous carbon, 90 % purity, a surface area between 250 and 300 $\text{m}^2 \text{ g}^{-1}$ and, according to the supplier, a density of $4.8 \times 10^{-2} \text{ g cm}^{-3}$.

To check consistency of primary characterization data for NC7000 with suppliers, structure and material size were investigated by transmission electron microscopy (TEM) with a Jeol 3010 (Tokyo, Japan), operating at 300 kV. TEM samples were prepared by deposition of a drop of NC7000 dispersion in ethanol, on a copper TEM grid, followed by evaporation at room temperature prior to analysis. Specific surface area was calculated by the Brunauer, Emmett, and Teller (BET) method (Brunauer et al. 1938), by nitrogen adsorption on a Micromeritics (Norcross, GA, USA) ASAP 2000 instrument at an adsorption temperature of $-196 \text{ }^\circ\text{C}$, after pre-treating the sample under high vacuum at $300 \text{ }^\circ\text{C}$ for 2 h.

ENMs dispersions preparation

Ultrapure water (minimum resistivity: 18.2 M Ω cm) was produced with a MilliQ water purifier system (Millipore, Bedford, MA, USA). The recommended reconstituted artificial freshwater (AFW) (OECD 1992), used for ecotoxicological testing, was prepared by dissolving $\text{CaCl}_2 \cdot 2\text{H}_2\text{O}$, $\text{MgSO}_4 \cdot 7\text{H}_2\text{O}$, NaHCO_3 , and KCl, in MilliQ water by magnetic stirring.

All inorganic salts were of analytical grade and purchased from Sigma-Aldrich (St. Louis, MI, USA). The physico-chemical characteristics of AFW were as follow: salinity was <1 ‰, ionic strength (IS) was 2 mmol l⁻¹, with Ca:Mg ions 4:1 and Na:K ions 10:1, acid capacity was 0.8 mmol l⁻¹, pH was 8 ± 0.3, and dissolved organic carbon (DOC) was <0.1 mg l⁻¹. A stock dispersion at the nominal concentration of 100 mg l⁻¹ in AFW was prepared from nanopowder and diluted to obtain working dispersions. According to different interactions between each ENM and the selected wavelength of the Dispersion Analyzer LUMiSizer[®] 651, P25, and NC7000 were tested at slightly different concentration levels as follows: 5, 10, 15, 20, 50, and 100 mg l⁻¹ for P25 and 10, 14, 20, 40, and 100 mg l⁻¹ for NC7000. The concentration range was selected according to ecotoxicological testing on ENMs and to the Limit of Detection (LOD) of LUMiSizer (i.e., 1 mg l⁻¹ for P25 and 0.1 mg l⁻¹ for NC7000). The temperature was set at 25 °C throughout the time span of analysis. Given the fast agglomeration and sedimentation of NC7000 in AFW (i.e., around 10 min) and according to Wang et al. (2013), 0.2 % w w⁻¹ of Humic Acid (Sigma-Aldrich, St. Louis, MI, USA) was used to increase the stability rate. Thus, according to the certificate of analysis of Humic Acid by Sigma-Aldrich, DOC of NC7000 dispersions was approx. 0.2 %. Each dispersion was homogenized with an ultrasonic bath (Falc Instruments s.r.l., Bergamo, Italy) at 50 kHz for 15 min immediately prior to sampling and analysis.

Short- and long-term stability of ENMs dispersions

The short-term stability of ENMs dispersions was assessed by DLS and ELS by means of a multi-angle Nicomp ZLS Z3000 (Particle Sizing System, Port Richey, FL, USA). The hydrodynamic diameter of P25 was measured over 1 h with an optical fiber set at 90° scattering angle, using a 25 mW laser, 639 nm wavelength, and an avalanche photodiode, able to increase the sensitivity and to multiply the signal intensity from scattered particles up to ten times. According to the physical principles of DLS, the intensity of light scattered by examined particles is assumed equal to that of an ideal sphere. Therefore, DLS was not suitable to calculate the hydrodynamic diameter of dispersed NC7000. The surface charge of

the electric double layer of both P25 and NC7000 was acquired with ELS, by calculating the phase shift of ENMs with the phase analysis light scattering (PALS). A 5 V electric field was applied and ζ-potential was determined from the mean phase shift with respect to time. The results from DLS and ELS were reported as an average of three measurements each.

Long-term (up to 30 days) stability of P25 and NC7000 dispersions was extrapolated by short-time (i.e., 33 min) measurements, carried out by the Multi-wavelength Dispersion Analyzer LUMiSizer[®] 651 (L.U.M. GmbH, Berlin, Germany), which is based on CSA. The LUMiSizer allows to speed up the separation of different components in dispersion by the application of a Relative Centrifugal Force (RCF), ranging from 5 to 2325, which accelerates the movement of materials compared to gravity. The wavelength of the transmitted light, through a polycarbonate quadratic synthetic cell with an optical path of 10 mm, was set at 470 nm. The transmission profiles obtained referred to the amount of light passing through the sample cell lying horizontally on the rotor over time [as shown by Fig. 1 in Detloff et al. (2007)]. Throughout each measurement with LUMiSizer, the progress of the transmission profiles moved from the lowest (red) to the highest (green) transmission values (Fig. 1). The variations of the transmission profiles over time and space provided information on the kinetics of the separation/sedimentation process, allowing to calculate the sedimentation rates of solid material.

Sedimentation of P25 and NC7000 dispersions was studied by selecting the transmittance (%) over time at the midpoint of the length of the cuvette, i.e., 117.48 mm far from the rotor, at different Rotation Per Minute (RPM; min⁻¹) and ENM initial concentrations tested. The midpoint of the cuvette was selected to obtain data comparable with the most common techniques (i.e., UV-Vis and ICP-MS) reported in literature. RPM was converted to RCF by the Eq. 1:

$$\text{RCF} = 1.1179 \times 10^{-3} \times \text{RPM}^2 \times R, \quad (1)$$

where R [m] is the radius, calculated from the center of the rotor to the point at which the transmittance values were considered. According to the Lambert–Beer's law, transmittance values were converted to absorbance and then to ENM concentration to finally plot concentration versus centrifugation time. The runtime

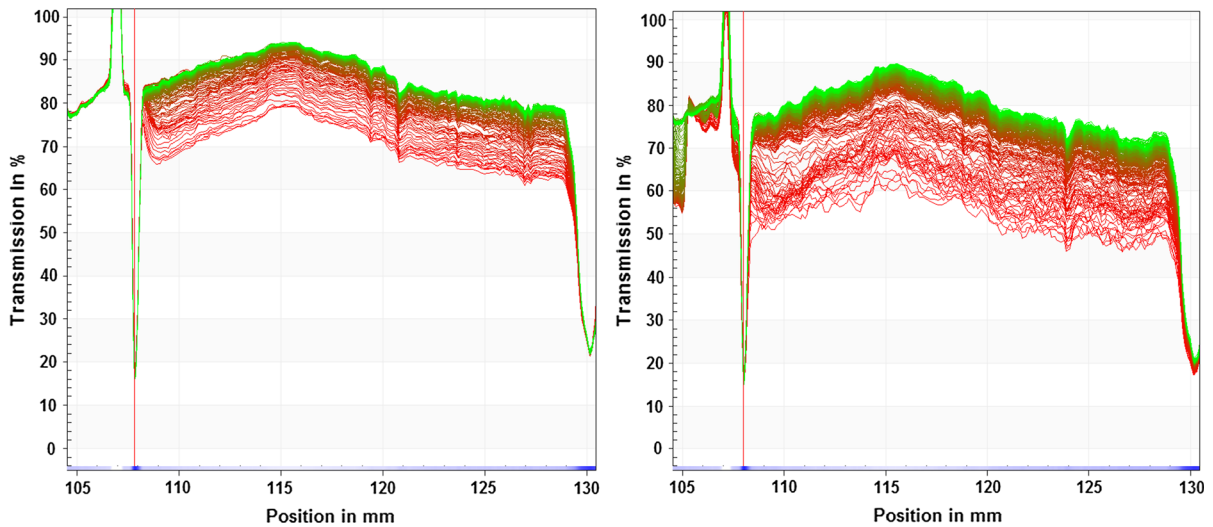


Fig. 1 Typical transmission profiles of n-TiO₂ P25 (*left*) and MWCNTs NC7000 (*right*) dispersions in AFW at 10 mg l⁻¹ at 1200 RPM

of each analysis was set at 2000s (i.e., 33.3 min), after proving that, regardless ENMs initial concentrations and RCF applied, this time interval was suitable to reach the plateau, i.e., the complete ENM sedimentation, resulting in ENM concentration in AFW = 0. The calculation of extrapolated day results from the following equation: centrifugation time × RCF. Each analysis was performed in triplicate and results were expressed as average. The collected data were interpreted by means of a first-order decay equation (Eq. 2), which was adapted from Brunelli et al. (2013) and Quik et al. (2014b).

$$C_t = (C_0 - \text{plateau}) \cdot e^{-kt} + \text{plateau}, \quad (2)$$

where C_t [mg l⁻¹] is the concentration at time t , C_0 [mg l⁻¹] is the initial concentration of ENM, k [s⁻¹] is the settling rate constant, t [s] is the settling time and plateau [mg l⁻¹] is the minimum concentration after centrifugation, corresponding to a constant value close to 0.

The estimation of the long-term (i.e., over 30 days) stability of ENMs was performed fitting the k values obtained at different RCF by LUMiSizer with linear regression, allowing to calculate k values at gravity. Finally, according to Quik et al. (2014b), sedimentation velocity of all dispersed ENMs was calculated by multiplying k with the sedimentation length (i.e., 9.48 mm, which was the length distance from the top

of the water surface to the midpoint of the cuvette). R software was used for data treatment.

Results and discussion

Before undertaking any stability experiment, the consistency of characterization data provided by suppliers was checked. According to Brunelli et al. (2013), n-TiO₂ showed a size distribution ranging from 10 to 65 nm (average: 27 nm), with partly irregular and semi-spherical particles. Anatase:rutile ratio was 4:1 ratio; specific surface area was 61 m² g⁻¹. As far as NC7000 is concerned, the diameter ranged from 4 to 16 nm (average: 8 nm) and the length from 575 to 3462 nm (average: 1543 nm) (Fig. S1). The specific surface area was 269 ± 13 m² g⁻¹. The overall characterization data obtained were consistent with those provided by the suppliers.

From short-time stability measurements to long-term stability estimation

The qualitative short-term stability assessment of ENMs dispersions was carried out over 1 h time, by measuring the hydrodynamic diameter of P25 and the ζ-potential of all the dispersions. The hydrodynamic

diameter of P25 increased from 480 nm to 2 μm , showing a fast particle agglomeration, as already observed in literature (Brunelli et al. 2013; Zhang et al. 2009). Moreover, ζ -potential was -4.7 ± 2.7 and -10.4 ± 1.9 , for P25 and NC7000 dispersions respectively, suggesting a general instability of the dispersions over the 0–1 h time interval.

The quantitative long-term stability of ENMs dispersions was estimated from short-time experiments by CSA–LUMiSizer instrumentation. The typical spatial range of settling data for dispersed ENMs was between the liquid/air phase boundary, at 108 mm far from the rotor of the centrifuge, corresponding to the top of the cuvette, and the bottom of the cell, at 130 mm. As an example, typical transmission profiles at 1200 RPM for P25 and NC7000 dispersions at 10 mg l^{-1} in AFW are presented in Fig. 1. Transmission profiles for P25 increased from an average of 69 %, representing the initial conditions, i.e., beginning of experiment, to 94 %, corresponding to the complete settling of particles (Fig. 1, left). As far as transmission profiles of NC7000 (Fig. 1, right) is concerned, the average transmission percentage spanned from 54 % to 83 %. The broader range of transmittance values obtained for NC7000 compared to P25 was a preliminary indication of a higher long-term stability of P25. Moving from transmittance to

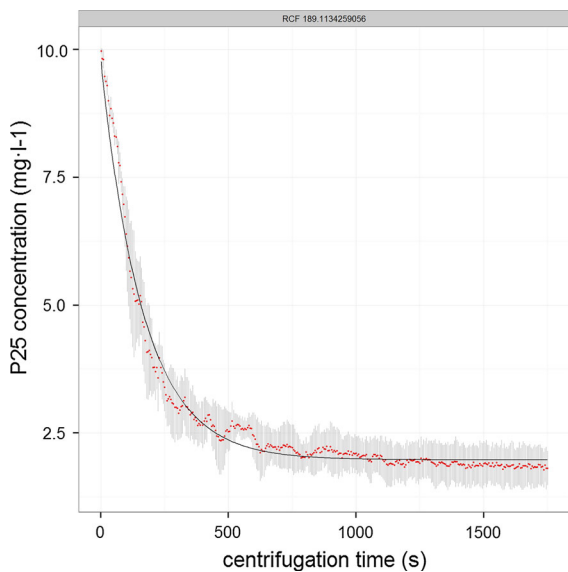


Fig. 2 Sedimentation profiles of n-TiO₂ P25 dispersed in AFW at 10 mg l^{-1} over centrifugation time at 189 RCF, corresponding to 1200 RPM

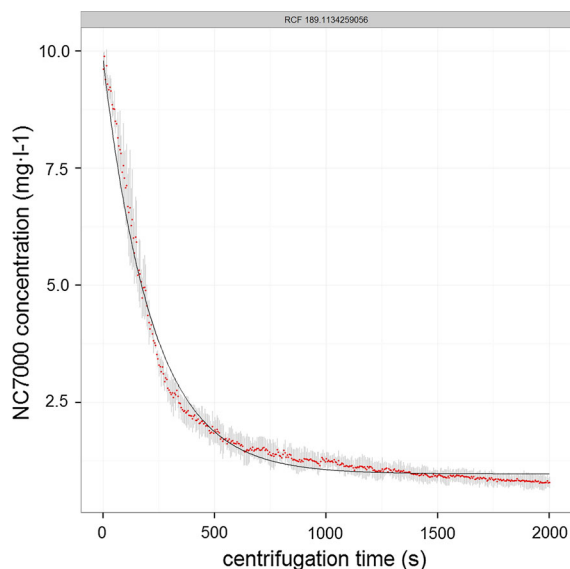


Fig. 3 Sedimentation profiles of MWCNTs NC7000 dispersed in AFW at 10 mg l^{-1} over centrifugation time at 189 RCF, corresponding to 1200 RPM

concentration, Figs. 2 and 3 show typical sedimentation behavior of P25 and NC7000 respectively, both dispersed in AFW at 10 mg l^{-1} , obtained by LUMiSizer at 189 RCF, corresponding to 1200 RPM. Equation 2 was used to describe experimental data (dots) with a first-order kinetic equation, to finally obtain sedimentation profiles with standard deviations (thin bar related to each dot). The overall sedimentation data of ENMs at different initial concentrations and RCF tested, are presented in Figs. S2–S11. The standard deviation over three measurements was inversely related to RCF applied and resulted higher for P25 than that of NC7000. Generally, as expected, by increasing RCF, sedimentation rate of ENMs increased, reaching the complete sedimentation, i.e., the plateau, over a shorter time. For example, as far as NC7000 dispersed at 10 mg l^{-1} is concerned (Fig. S7), the complete sedimentation was obtained after approx. 150 s of analysis at 820 RCF compared to 2000s of analysis at 84 RCF. Equation 2 was used to calculate the first-order rate constant (k) values at different RCF selected, and the results are displayed in Figs. 4, 5. The overall data fitted well with linear regression and, therefore, rate constant k at gravity, i.e., the slope of each line, was calculated for all dispersions. The fitting line was forced to pass through the origin, assuming that at $\text{RCF} = 0$, $k = 0$.

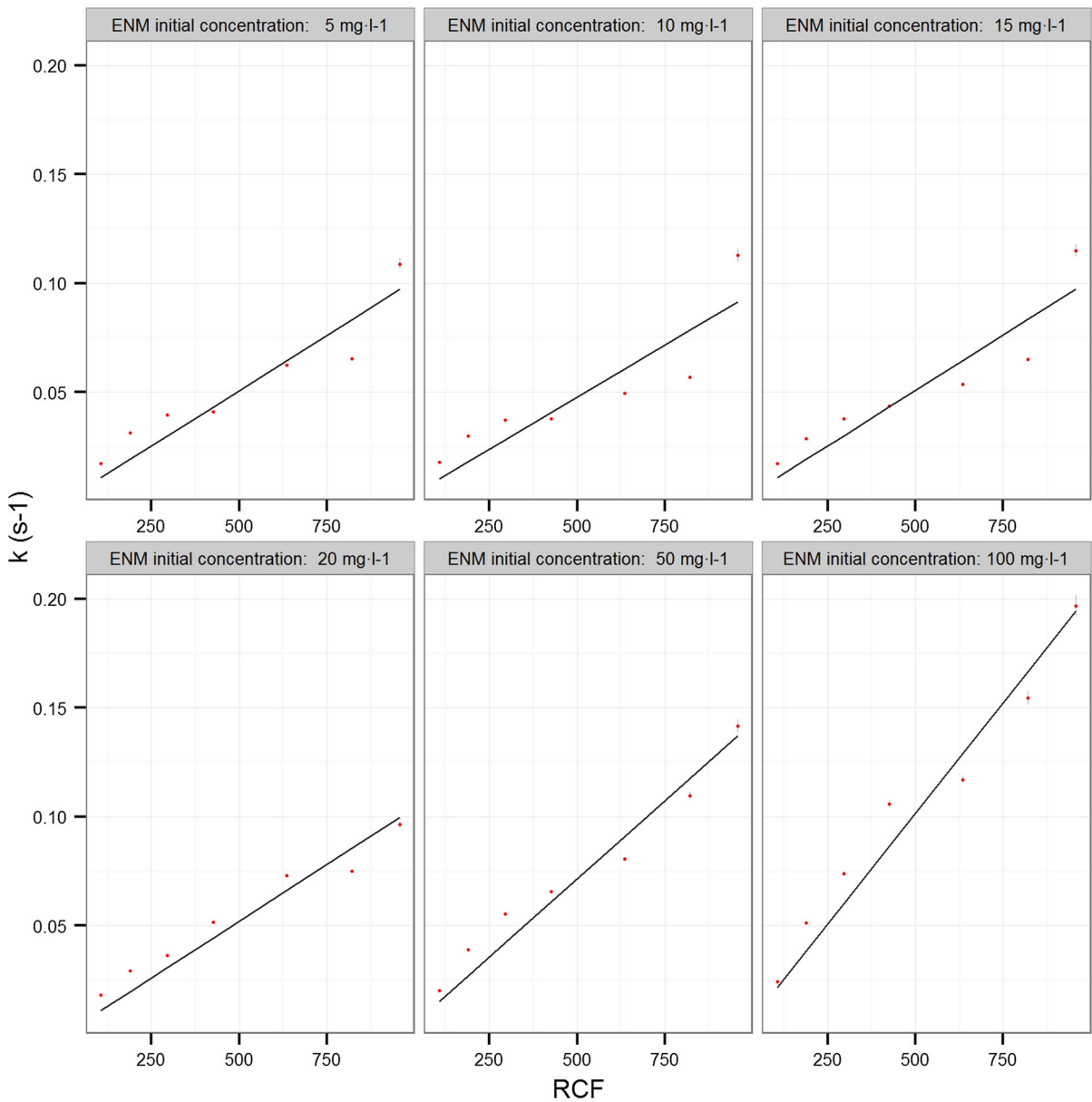


Fig. 4 *k* values (dots) and linear fitting (line) of dispersed P25, calculated at different initial concentrations and RCF

The estimated *k* values at gravity, the correlation coefficients (R^2) of the fitting as well as the sedimentation velocity data are summarized in Table 1. Standard deviations of *k* were between one and two order of magnitude lower than the average *k* values. R^2 resulted satisfactorily for all the dispersions, ranging from 0.918 to 0.989 (0.972 ± 0.02 for P25 and 0.958 ± 0.02 for NC7000). In general, *k* spanned one order of magnitude, ranging from 7.21×10^{-5} to

4.12×10^{-4} , increasing with the increase of initial ENMs concentration, except for P25 dispersed at 10 mg l^{-1} . Finally, the comparison of sedimentation behavior between P25 and NC7000 dispersions is presented in Fig. 6. Generally, as expected from a preliminary observation of transmission profiles displayed in Fig. 1, a higher stability of P25 dispersions in comparison with NC7000 dispersions was found, especially for concentrations above 20 mg l^{-1} .

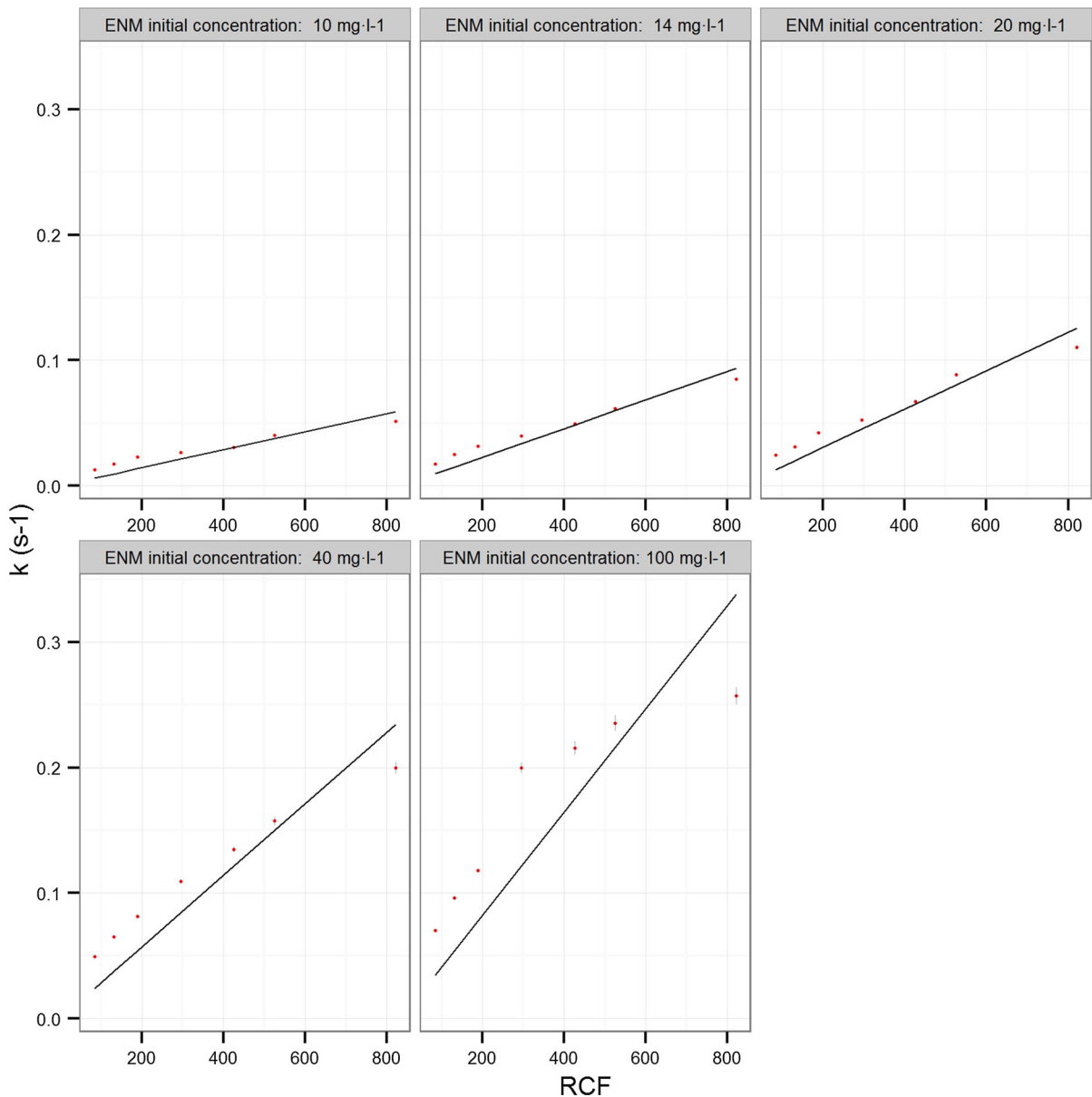


Fig. 5 k values (dots) and linear fitting (line) of dispersed NC7000, calculated at different initial concentrations and RCF

Comparison of the estimated long-term stability with previous results

Schwytzer et al. (2012) and Adeleye and Keller (2014) were the only authors who investigated the long-term (up to 140 days) stability of several carbon nanotubes under different environmental conditions, but no sedimentation kinetics were provided. A few studies have investigated the

sedimentation behavior of ENMs at environmental realistic concentrations (Brunelli et al. 2013) or tested ENMs with different chemical composition and surface area but with similar shape (Keller et al. 2010), for no longer than 15 days and using two different techniques, i.e., molecular spectroscopy for organic samples and mass spectrometry for inorganic samples (Quik et al. 2014b; Van Koetsem et al. 2015).

Table 1 First-order fitting equation parameters and sedimentation velocity data for P25 and NC7000 dispersions at different initial concentrations tested in AFW

ENM	Initial ENM concentration (mg l ⁻¹)	<i>k</i> (s ⁻¹) at force gravity	SD	<i>R</i> ²	Sedimentation velocity (m day ⁻¹)
P25	5	1.02 × 10 ⁻⁴	7.35 × 10 ⁻⁶	0.969	8.35 × 10 ⁻²
	10	9.55 × 10 ⁻⁵	9.84 × 10 ⁻⁶	0.940	7.82 × 10 ⁻²
	15	1.02 × 10 ⁻⁴	8.34 × 10 ⁻⁶	0.961	8.35 × 10 ⁻²
	20	1.04 × 10 ⁻⁴	5.32 × 10 ⁻⁶	0.985	8.52 × 10 ⁻²
	50	1.43 × 10 ⁻⁴	6.27 × 10 ⁻⁶	0.989	1.17 × 10 ⁻¹
	100	2.03 × 10 ⁻⁴	8.68 × 10 ⁻⁶	0.989	1.66 × 10 ⁻¹
NC7000	10	7.21 × 10 ⁻⁵	6.17 × 10 ⁻⁶	0.958	5.90 × 10 ⁻²
	14	1.14 × 10 ⁻⁴	7.09 × 10 ⁻⁶	0.977	9.34 × 10 ⁻²
	20	1.53 × 10 ⁻⁴	1.03 × 10 ⁻⁵	0.974	1.25 × 10 ⁻¹
	40	2.85 × 10 ⁻⁴	2.34 × 10 ⁻⁵	0.961	2.33 × 10 ⁻¹
	100	4.12 × 10 ⁻⁴	5.01 × 10 ⁻⁵	0.918	3.37 × 10 ⁻¹

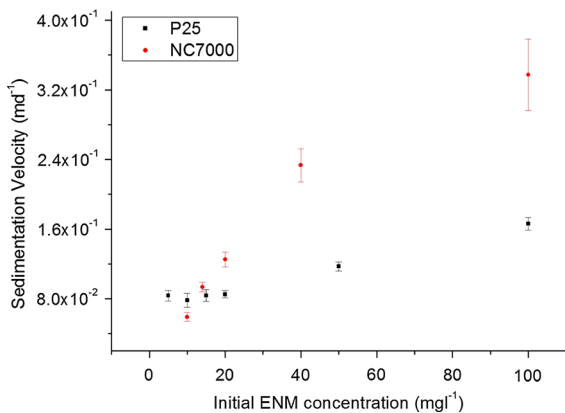


Fig. 6 Sedimentation velocity data, obtained by LUMiSizer, for P25 (black squares) and NC7000 (red points) at the following initial ENMs concentrations: 5, 10, 15, 20, 50, and 100 mg l⁻¹ for P25 and 10, 14, 20, 40, and 100 mg l⁻¹ for NC7000

In very few studies the stability of nano-based dispersions was investigated by CSA–LUMiSizer instrumentation, by qualitatively comparing the sedimentation behavior of ENMs (Erné 2012; Krause et al. 2010; Sobisch et al. 2010, 2012; Lerche 2002). DeLoid et al. (2014) proposed a quantitative approach based on CSA, calculating sedimentation coefficient distributions (Supplementary Fig. 2 in DeLoid et al. 2014) and diffusion rates of ENMs in culture media for in vitro dosimetry, using the CSA–analytical ultracentrifugation, a relatively expensive and time-consuming technique.

The results obtained in this work with LUMiSizer were compared with data collected from the only studies reporting sedimentation kinetics for n-TiO₂ and MWCNTs, i.e., Quik et al. (2014b) and our previous work (Brunelli et al. 2013). Table 2 summarizes all the sedimentation velocity data and the experimental conditions available in the literature. Specifically, as far as TiO₂ is concerned, Battin et al. (2009), Keller et al. (2010), and Brunelli et al. (2013) studied the sedimentation behavior of P25 in several waters. As far as carbon-based materials are concerned, Adeleye and Keller (2014), Schwyzer et al. (2012), and Kennedy et al. (2008) investigated the sedimentation behavior of MWCNTs, while in Quik et al. (2014b) the dispersion stability of a spherical carbon-based ENM, i.e., fullerene C₆₀, was studied. Although there are many differences among the compared studies with regards to ENM’s type, initial ENM concentration, medium, analytical technique, and experimental duration, sedimentation velocity data presented in this work are in good agreement with data reported in Table 2. More specifically, sedimentation velocity data of P25 dispersions extrapolated from LUMiSizer, shown in Table 1, span a higher range, i.e., from 7.82 × 10⁻² to 1.66 × 10⁻¹ m day⁻¹, compared to literature data in freshwater (Table 2). Vice versa, as far as NC7000 is concerned, sedimentation velocity data in Table 1 comprised in a narrower range compared to Kennedy et al. (2008), i.e., from 5.9 × 10⁻² to 3.37 × 10⁻¹ m day⁻¹ for

Table 2 Sedimentation velocity and experimental conditions from literature (Brunelli et al. 2013; Quik et al. 2014b)

Reference	Tested ENM	Sedimentation velocity ($\text{m} \times \text{day}^{-1}$)	ENM initial concentrations	Medium	Experiment time
Quik et al. 2014a, b	C ₆₀ n-CeO ₂ n-SiO ₂ -Ag PVP n-Ag	8.8×10^{-2} 5.4×10^{-3} 2.4×10^{-3} 8.2×10^{-4}	0.5, 2.5 and $10 \text{ mg} \times \text{l}^{-1}$ for the metal ENMs and 5, 25 and 100 mg l^{-1} for C ₆₀	Freshwater lake	15 days
Brunelli et al. 2013	n-TiO ₂ P25	$3.5 \times 10^{-3} < x < 2 \times 10^{-2}$	0.01, 0.1, 1, and $10 \text{ mg} \times \text{l}^{-1}$	Artificial freshwater according to ASTM E729-96, 2004 (2007)	50 h
Chinnapongse et al. 2012	n-CeO ₂	$10^{-2} < x < 10^{-1}$	1, 10 and 100 mg l^{-1}	River waters	12 days
Chinnapongse et al. 2011	Citrate capped n-Ag	$10^{-2} < x < 10^{-1}$	$1.5 \times 10^{-5} \text{ mg l}^{-1}$	Natural freshwater	48 h
Quik et al. 2010	n-CeO ₂	$10^{-2} < x < 10^{-1}$	10 mg l^{-1}	Algae growth medium according to OECD (2006)	12 days
Keller et al. 2010	n-TiO ₂ P25 n-ZnO n-CeO ₂	$5 \times 10^{-4} < x < 7 \times 10^{-2}$ $3 \times 10^{-4} < x < 8 \times 10^{-2}$ $3 \times 10^{-3} < x < 5 \times 10^{-2}$	10, 50, 100 and 200 mg l^{-1}	Synthetic and real sea and freshwaters, lagoon, river and groundwater	6 h
Kennedy et al. 2008	MWCNTs	$2 \times 10^{-1} < x < 1.2$	100 mg l^{-1}	Moderately hard reconstituted freshwater according U.S. Environmental Protection Agency (2002)	2 h
Battin et al. 2009	n-TiO ₂ P25 n-TiO ₂ Hombikat UV100	$10^{-1} < x < 3 \times 10^{-1}$	5.3 mg l^{-1}	Natural lake water	7 h

NC7000 instead of 3×10^{-1} and 1.2 m day^{-1} , respectively, while Quik et al. (2014b) obtained $8.8 \times 10^{-2} \text{ m day}^{-1}$ for fullerene C₆₀ in freshwater lake. In conclusion, it can be stated that small difference among our data and literature results can be ascribed to the type of ENM, to the dispersion medium, to the experimental time investigated as well as to the range of the concentrations tested.

Conclusions

The stability of ENMs dispersions is generally affected by the intrinsic physico-chemical properties of ENMs, dispersion conditions (e.g., pH, ionic strength, salt content and valence of cations, dissolved organic carbon, natural organic matter), initial ENMs concentration, and transformations in the environment

(e.g., homo- and hetero-aggregation/agglomeration, sedimentation, dissolution, degradation). We have proved that speeding up the settling velocity up to 960 times the one at gravity, applied to ENMs dispersed in freshwater, with fixed pH (8 ± 0.3), IS (2 mmol l^{-1}), and DOC ($\leq 0.2 \text{ mg l}^{-1}$), provided consistent and reproducible results. Thus, it was demonstrated that the long-term stability of ENMs dispersions can be quantitatively predicted by means of short-time experiments, typically from few minutes to half hour. The methodology presented here can be extended to investigate which individual parameter (e.g., size, shape, surface charge, chemical composition etc.) is most affecting the stability of ENMs in natural and/or biological media. This would greatly improve the interpretation of in vitro and in vivo toxicological effects, and support the modeling of environmental ENMs fate and transport.

Acknowledgments This research was partially funded by the European Commission within the Seventh Framework Program (FP7; SUN project - Grant Agreement n° 604305). The authors thankfully acknowledge VenetoNanotech for providing TEM images of MWCNT and Riccardo Cossi (Qi srl, Pomezia, Italy) and Andrea Scandella (University Ca' Foscari of Venice) for their valuable technical support.

Compliance with ethical standards

Conflict of Interest The authors declare that they have no conflict of interest.

References

- Adeleye AS, Keller AA (2014) Long-term colloidal stability and metal leaching of single wall carbon nanotubes: effect of temperature and extracellular polymeric substances. *Water Res* 49:236–250. doi:[10.1016/j.watres.2013.11.032](https://doi.org/10.1016/j.watres.2013.11.032)
- Afroz ARMN, Khan IA, Hussain SM, Saleh NB (2013) Mechanistic heteroaggregation of gold nanoparticles in a wide range of solution chemistry. *Environ Sci Technol* 47:1853–1860
- Al-Kattan A, Wichser A, Zuin S et al (2014) Behavior of TiO₂ released from Nano-TiO₂-containing paint and comparison to pristine nano-TiO₂. *Environ Sci Technol* 48:6710–6718. doi:[10.1021/es5006219](https://doi.org/10.1021/es5006219)
- Arvidsson R, Molander S, Sandén BA, Hassellöv M (2011) Challenges in exposure modeling of nanoparticles in aquatic environments. *Hum Ecol Risk Assess* 17:245–262
- ASTM E729-96, 2004 (2007) Standard guide for conducting acute toxicity testing on test materials with fishes, macroinvertebrates, and amphibians. ASTM International, West Conshohocken. doi:[10.1520/E0729-96R07](https://doi.org/10.1520/E0729-96R07)
- Battin TJ, Kammer FV, Weilharter A et al (2009) Nanostructured TiO₂: transport behavior and effects on aquatic microbial communities under environmental conditions. *Environ Sci Technol* 43:8098–8104. doi:[10.1021/es9017046](https://doi.org/10.1021/es9017046)
- Brunauer S, Emmett PH, Teller E (1938) Adsorption of gases in multimolecular layers. *J Am Chem Soc* 60:309–319
- Brunelli A, Pojana G, Callegaro S, Marcomini A (2013) Agglomeration and sedimentation of titanium dioxide nanoparticles (n-TiO₂) in synthetic and real waters. *J Nanopart Res* 15:1–10
- Buettner KM, Rinciog CI, Mylon SE (2010) Aggregation kinetics of cerium oxide nanoparticles in monovalent and divalent electrolytes. *Colloid Surf A Physicochem Eng Asp* 366:74–79. doi:[10.1016/j.colsurfa.2010.05.024](https://doi.org/10.1016/j.colsurfa.2010.05.024)
- Chen KL, Elimelech M (2006) Aggregation and deposition kinetics of fullerene (C60) nanoparticles. *Langmuir* 22:10994–11001
- Chinnapongse SL, MacCuspie RI, Hackley VA (2011) Persistence of singly dispersed silver nanoparticles in natural freshwaters, synthetic seawater, and simulated estuarine waters. *Sci Total Environ* 409:2443–2450. doi:[10.1016/j.scitotenv.2011.03.020](https://doi.org/10.1016/j.scitotenv.2011.03.020)
- Chowdhury I, Duch MC, Mansukhani ND et al (2013) Colloidal properties and stability of graphene oxide nanomaterials in the aquatic environment. *Environ Sci Technol* 47:6288–6296
- Dahirel V, Jardat M (2010) Effective interactions between charged nanoparticles in water: what is left from the DLVO theory? *Curr Opin Colloid Interface Sci* 15:2–7. doi:[10.1016/j.cocis.2009.05.006](https://doi.org/10.1016/j.cocis.2009.05.006)
- DeLoid G, Cohen JM, Darrah T et al (2014) Estimating the effective density of engineered nanomaterials for in vitro dosimetry. *Nat Commun* 5:3514. doi:[10.1038/ncomms4514](https://doi.org/10.1038/ncomms4514)
- Detloff T, Sobisch T, Lerche D (2007) Particle size distribution by space or time dependent extinction profiles obtained by analytical centrifugation (concentrated systems). *Powder Technol* 174:50–55
- Erné B (2012) Sedimentation equilibria of colloidal dispersions in ultrathin glass capillaries. *Dispers Lett* 3:16–17
- Farré M, Gajda-Schranz K, Kantiani L et al (2009) Ecotoxicity and analysis of nanomaterials in the aquatic environment. *Anal Bioanal Chem* 393:81–95. doi:[10.1007/s00216-008-2458-1](https://doi.org/10.1007/s00216-008-2458-1)
- Gambinossi F, Mylon SE, Ferri JK (2015) Aggregation kinetics and colloidal stability of functionalized nanoparticles. *Adv Colloid Interfac* 222:332–349. doi:[10.1016/j.cis.2014.07.015](https://doi.org/10.1016/j.cis.2014.07.015)
- Gottschalk F, Sonderer T, Scholz RW, Nowack B (2010) Possibilities and limitations of modeling environmental exposure to engineered nanomaterials by probabilistic material flow analysis. *Environ Toxicol Chem* 29:1036–1048
- Hartmann NB, Skjolding LM, Hansen SF et al (2014) Environmental fate and behaviour of nanomaterials. The Danish Environmental Protection Agency, Copenhagen
- Hotze EM, Phenrat T, Lowry GV (2010) Nanoparticle aggregation: challenges to understanding transport and reactivity in the environment. *J Environ Qual* 39:1909–1924
- Hunter RJ (1988) Zeta potential in colloidal science—principles and applications, 3rd edn. Academic Press Limited, London
- Jarvie HP, Al-Obaidi H, King SM et al (2009) Fate of silica nanoparticles in simulated primary wastewater treatment. *Environ Sci Technol* 43:8622–8628. doi:[10.1021/es901399q](https://doi.org/10.1021/es901399q)
- Jiang J, Oberdörster G, Biswas P (2009) Characterization of size, surface charge, and agglomeration state of nanoparticle dispersions for toxicological studies. *J Nanopart Res* 11:77–89. doi:[10.1007/s11051-008-9446-4](https://doi.org/10.1007/s11051-008-9446-4)
- Keller AA, Wang H, Zhou D et al (2010) Stability and aggregation of metal oxide nanoparticles in natural aqueous matrices. *Environ Sci Technol* 44:1962–1967
- Kennedy Alan J, Hull MS, Steevens JA et al (2008) Factors influencing the partitioning and toxicity of nanotubes in the aquatic environment. *Environ Toxicol Chem* 27:1932–1941. doi:[10.1897/07-624.1](https://doi.org/10.1897/07-624.1)
- Krause B, Mende M, Potschke P et al (2010) Dispersability and particle size distribution of CNTs in an aqueous surfactant dispersion as a function of ultrasonic treatment time. *Carbon* 48:2746–2754. doi:[10.1016/j.carbon.2010.04.002](https://doi.org/10.1016/j.carbon.2010.04.002)
- Lerche D (2002) Dispersion stability and particle characterization by sedimentation kinetics in a centrifugal field. *J Dispers Sci Technol* 23:699–709. doi:[10.1081/DIS-120015373](https://doi.org/10.1081/DIS-120015373)
- Liu J, Hurt RH (2010) Ion release kinetics and particle persistence in aqueous nano-silver colloids. *Environ Sci Technol* 44:2169–2175. doi:[10.1021/es9035557](https://doi.org/10.1021/es9035557)

- Liu HH, Surawanvijit S, Rallo R et al (2011a) Analysis of nanoparticle agglomeration in aqueous suspensions via constant-number monte carlo simulation. *Environ Sci Technol* 45:9284–9292. doi:[10.1021/es202134p](https://doi.org/10.1021/es202134p)
- Liu X, Wazne M, Chou T et al (2011b) Influence of Ca²⁺ and Suwannee River humic acid on aggregation of silicon nanoparticles in aqueous media. *Water Res* 45:105–112. doi:[10.1016/j.watres.2010.08.022](https://doi.org/10.1016/j.watres.2010.08.022)
- Liu J, Legros S, Ma G et al (2012) Influence of surface functionalization and particle size on the aggregation kinetics of engineered nanoparticles. *Chemosphere* 87:918–924
- Loux NT, Su YS, Hassan SM (2011) Issues in assessing environmental exposures to manufactured nanomaterials. *Int J Environ Res Public Health* 8:3562–3578
- Lowry GV, Hotze EM, Bernhardt ES et al (2010) Environmental occurrences, behavior, fate, and ecological effects of nanomaterials: an introduction to the special series. *J Environ Qual* 39:1867–1874
- Mueller NC, Nowack B (2008) Exposure modeling of engineered nanoparticles in the environment. *Environ Sci Technol* 42:4447–4453
- Nowack B, Ranville JF, Diamond S et al (2012) Potential scenarios for nanomaterial release and subsequent alteration in the environment. *Environ Toxicol Chem* 31:50–59
- Nowack B, Mueller N, Krug H, Wick P (2014) How to consider engineered nanomaterials in major accident regulations? *Environ Sci Eur* 26:2
- OECD (1992) Guidelines for Testing of Chemicals No. 203. Fish, Acute Toxicity Test (Annex 2 Composition of the recommended reconstituted water). OECD, Paris
- OECD (2006) Freshwater alga and cyanobacteria, growth inhibition test. Organisation for Economic Co-Operation and Development, Paris
- Pettitt ME, Lead JR (2013) Minimum physicochemical characterisation requirements for nanomaterial regulation. *Environ Int* 52:41–50
- Phenrat T, Saleh N, Sirk K et al (2006) Aggregation and sedimentation of aqueous nanoscale zerovalent iron dispersions. *Environ Sci Technol* 41:284–290. doi:[10.1021/es061349a](https://doi.org/10.1021/es061349a)
- Piccinno F, Gottschalk F, Seeger S, Nowack B (2012) Industrial production quantities and uses of ten engineered nanomaterials in Europe and the world. *J Nanopart Res* 14:1–11. doi:[10.1007/s11051-012-1109-9](https://doi.org/10.1007/s11051-012-1109-9)
- Praetorius A, Scheringer M, Hungerbühler K (2012) Development of environmental fate models for engineered nanoparticles—a case study of TiO₂ nanoparticles in the Rhine river. *Environ Sci Technol* 46:6705–6713
- Quik JTK, Lynch I, Hoecke KV et al (2010) Effect of natural organic matter on cerium dioxide nanoparticles settling in model fresh water. *Chemosphere* 81:711–715. doi:[10.1016/j.chemosphere.2010.07.062](https://doi.org/10.1016/j.chemosphere.2010.07.062)
- Quik JTK, Vonk JA, Hansen SF et al (2011) How to assess exposure of aquatic organisms to manufactured nanoparticles? *Environ Int* 37:1068–1077
- Quik JTK, Stuart MC, Wouterse M et al (2012) Natural colloids are the dominant factor in the sedimentation of nanoparticles. *Environ Toxicol Chem* 31:1019–1022. doi:[10.1002/etc.1783](https://doi.org/10.1002/etc.1783)
- Quik JTK, van De Meent D, Koelmans AA (2014a) Simplifying modeling of nanoparticle aggregation–sedimentation behavior in environmental systems: a theoretical analysis. *Water Res* 62:193–201. doi:[10.1016/j.watres.2014.05.048](https://doi.org/10.1016/j.watres.2014.05.048)
- Quik JTK, Velzeboer I, Wouterse M et al (2014b) Heteroaggregation and sedimentation rates for nanomaterials in natural waters. *Water Res* 48:269–279. doi:[10.1016/j.watres.2013.09.036](https://doi.org/10.1016/j.watres.2013.09.036)
- Ramsden CS, Henry TB, Handy RD (2013) Sub-lethal effects of titanium dioxide nanoparticles on the physiology and reproduction of zebrafish. *Aquat Toxicol* 126:404–413. doi:[10.1016/j.aquatox.2012.08.021](https://doi.org/10.1016/j.aquatox.2012.08.021)
- Schwarzer H-C, Peukert W (2005) Prediction of aggregation kinetics based on surface properties of nanoparticles. *Chem Eng Sci* 60:11–25
- Schwyzler I, Kaegi R, Sigg L et al (2012) Long-term colloidal stability of 10 carbon nanotube types in the absence/presence of humic acid and calcium. *Environ Pollut* 169:64–73
- Sobisch T, Kuechler S, Uhl A (2010) Comprehensive characterization of medical nutrition—accelerated stability analysis and creaming velocity distribution. *Dispers Lett* 1:10–13
- Sobisch T, Le Coeur C, Larue O et al (2012) Characterization of sedimentation and consolidation behaviour of kaolin suspensions in presence of dispersant. *Dispers Lett* 3:18–22
- Suttiponparmit K, Jiang J, Sahu M et al (2011) Role of surface area, primary particle size, and crystal phase on titanium dioxide nanoparticle dispersion properties. *Nanoscale Res Lett* 6:27
- Takeuchi Y, Ida T, Kimura K (1997) Colloidal stability of gold nanoparticles in 2-propanol under laser irradiation. *J Phys Chem B* 101:1322–1327. doi:[10.1021/jp963107a](https://doi.org/10.1021/jp963107a)
- Tiraferri A, Chen KL, Sethi R, Elimelech M (2008) Reduced aggregation and sedimentation of zero-valent iron nanoparticles in the presence of guar gum. *J Colloid Interface Sci* 324:71–79. doi:[10.1016/j.jcis.2008.04.064](https://doi.org/10.1016/j.jcis.2008.04.064)
- U.S. Environmental Protection Agency (2002) Methods for measuring the acute toxicity of effluents and receiving waters to freshwater and marine organisms. EPA/812/R/02/012. Office of Water, Washington, DC
- Van der Zande BMI, Dhont JKG, Bohmer MR, Philipse AP (2000) Colloidal dispersions of gold rods characterized by dynamic light scattering and electrophoresis. *Langmuir* 16:459–464
- Van Koetsem F, Verstraete S, Van der Meeren P, Du Laing G (2015) Stability of engineered nanomaterials in complex aqueous matrices: settling behaviour of CeO₂ nanoparticles in natural surface waters. *Environ Res* 142:207–214. doi:[10.1016/j.envres.2015.06.028](https://doi.org/10.1016/j.envres.2015.06.028)
- Villarreal FD, Das GK, Abid A et al (2014) Sublethal effects of CuO nanoparticles on *Mozambique tilapia (Oreochromis mossambicus)* are modulated by environmental salinity. *PLoS ONE* 9:e88723. doi:[10.1371/journal.pone.0088723](https://doi.org/10.1371/journal.pone.0088723)
- Wang F, Yao J, Chen H et al (2013) Sorption of humic acid to functionalized multi-walled carbon nanotubes. *Environ Pollut* 180:1–6. doi:[10.1016/j.envpol.2013.04.035](https://doi.org/10.1016/j.envpol.2013.04.035)
- Wiesner MR, Lowry GV, Jones KL et al (2009) Decreasing Uncertainties in assessing environmental exposure, risk, and ecological implications of nanomaterials†‡. *Environ Sci Technol* 43:6458–6462. doi:[10.1021/es803621k](https://doi.org/10.1021/es803621k)
- Zhang Y, Yang M, Portney N et al (2008) Zeta potential: a surface electrical characteristic to probe the interaction of nanoparticles with normal and cancer human breast

- epithelial cells. *Biomed Microdevices* 10:321–328. doi:[10.1007/s10544-007-9139-2](https://doi.org/10.1007/s10544-007-9139-2)
- Zhang Y, Chen Y, Westerhoff P, Crittenden J (2009) Impact of natural organic matter and divalent cations on the stability of aqueous nanoparticles. *Water Res* 43:4249–4257. doi:[10.1016/j.watres.2009.06.005](https://doi.org/10.1016/j.watres.2009.06.005)
- Zhang W, Crittenden J, Li K, Chen Y (2012) Attachment efficiency of nanoparticle aggregation in aqueous dispersions: modeling and experimental validation. *Environ Sci Technol* 46:7054–7062